**Supplementary Material**

# Timing of iceberg scours and massive ice-rafting events in the subtropical North Atlantic

Alan Condron[1*] and Jenna Hill[2]

[1]*Geology and Geophysics, Woods Hole Oceanographic Institution, Woods Hole, MA 02543, USA*

[2]*United States Geological Survey, Pacific Coastal & Marine Science Center Santa Cruz, CA 95005, USA*

*corresponding author: acondron@whoi.edu

**Contents:**

**Information on Supplementary Downloadable Data Files**

**Dataset1: Helpful files for plotting and reading binary data**
**XG.data:** model longitude grid points (for plotting the binary output on a map projection)
**YG.data:** model latitude grid points (for plotting the binary output on a map projection)
**readbin.m:** Matlab script for reading all binary files. See comments below.

**Dataset2: Data displayed in Figure 2**
**fig2_jan_SST.data:** Sea surface temperature data (deg. C) for fig 2a.
**fig2_sept_SST.data:** Sea surface temperature data (deg. C) for fig 2b.
**fig2_jan_uvel.data:** u (zonal) component of surface ocean velocity (m/s) for fig. 2a
**fig2_jan_vvel.data:** v (meridional) component of surface velocity (m/s) for fig. 2a
**fig2_sept_uvel.data:** u (zonal) component of surface ocean velocity (m/s) for fig. 2b
**fig2_sept_vvel.data:** v (meridional) component of surface velocity (m/s) for fig. 2b

**Dataset3: Data displayed in Figure 6**
**fig6_iceberg_density.txt**: Iceberg density data displayed in Figure 6. 3 column table.

**Dataset4: Data displayed in Figure 7**
**fig7_iceberg_locations.txt:** Longitude/latitude locations of the icebergs displayed in Figure 7a-d.
**fig7_SSS_PanelA.data:** Sea surface salinity (SSS) data displayed in fig7a.
**fig7_SSS_PanelB.data:** Sea surface salinity (SSS) data displayed in fig7b.
**fig7_SSS_PanelC.data:** Sea surface salinity (SSS) data displayed in fig7c.
**fig7_SSS_PanelD.data:** Sea surface salinity (SSS) data displayed in fig7d.

**Dataset5: Data displayed in Figure 8**
**fig8_SST_PanelA.data:** Sea surface temperature (SST) data displayed in fig8a.
**fig8_SST_PanelB.data:** Sea surface temperature (SST) data displayed in fig8b.
**fig8_SST_PanelC.data:** Sea surface temperature (SST) data displayed in fig8c.
**fig8d_SST_timeseries.txt:** Time series of sea surface temperature shown in Fig 8d

**Dataset6: Data displayed in Figure 9**
**fig9_iceberg_scour_data.txt:** latitude and depth of the iceberg scours show in Fig 9

**Notes:** Data files ending '.data' are in binary format with 4-byte precision (real*4). All binary files (including the grid files) are two dimensional and are 3060x510 grid points in size. These files are all on the model's native grid with a spatial resolution of ~18km (1/6 deg.). The binary files can be read using the included MATLAB routine, readbin.m. For example, to read the sea surface salinity data in file 'fig7_SSS_PanelA.data', in the Matlab command line type: sss=readbin('SSS.fig1_control.data', [3060 510]);

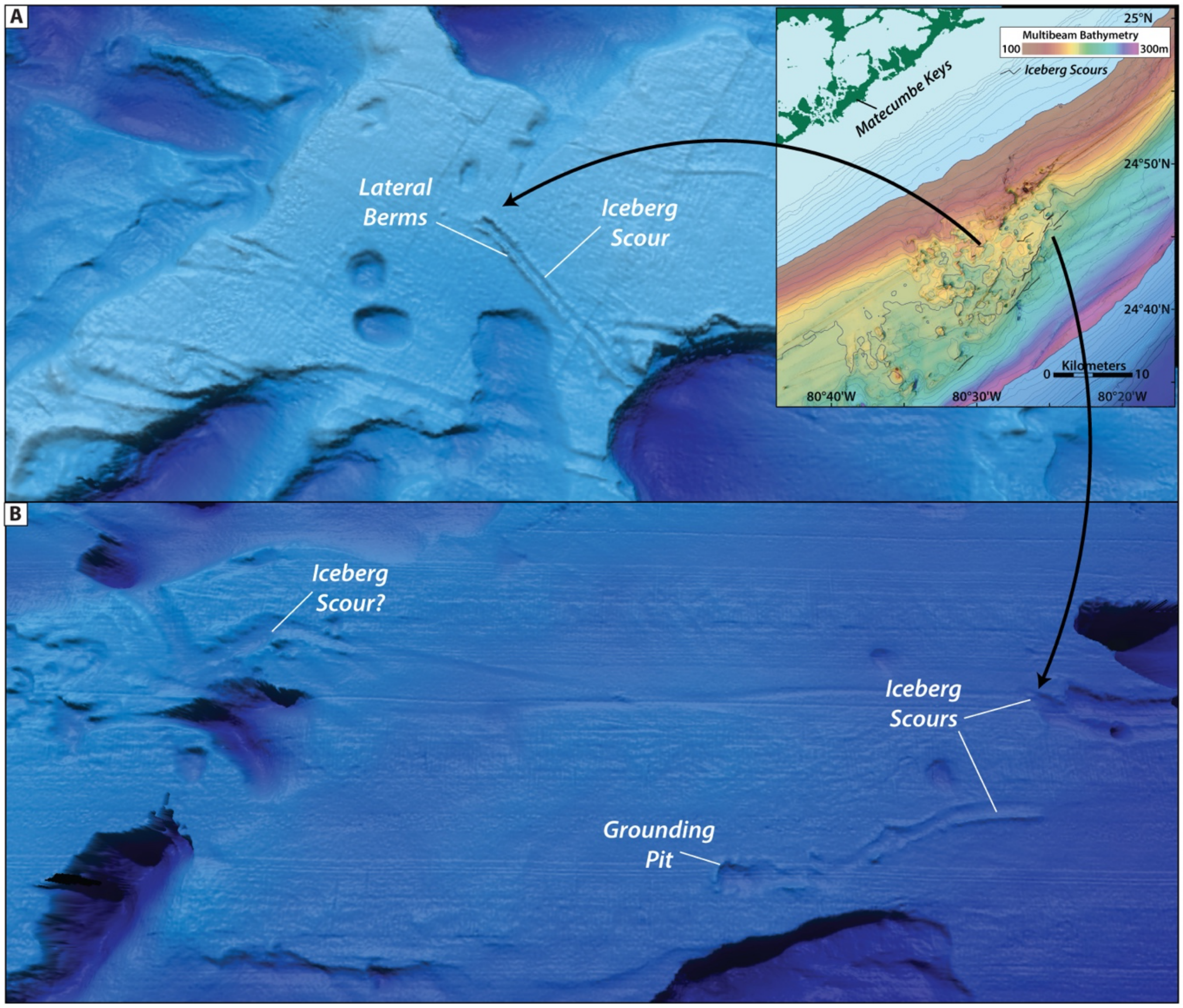


**Supplementary Figure 1:** Seafloor iceberg scours are observed as far south as the Florida Keys, with characteristic iceberg plough mark morphologies: (A) Lateral berms, interpreted as iceberg push-up ridges; (B) Terminal grounding pits indicate where icebergs came to rest on the seafloor

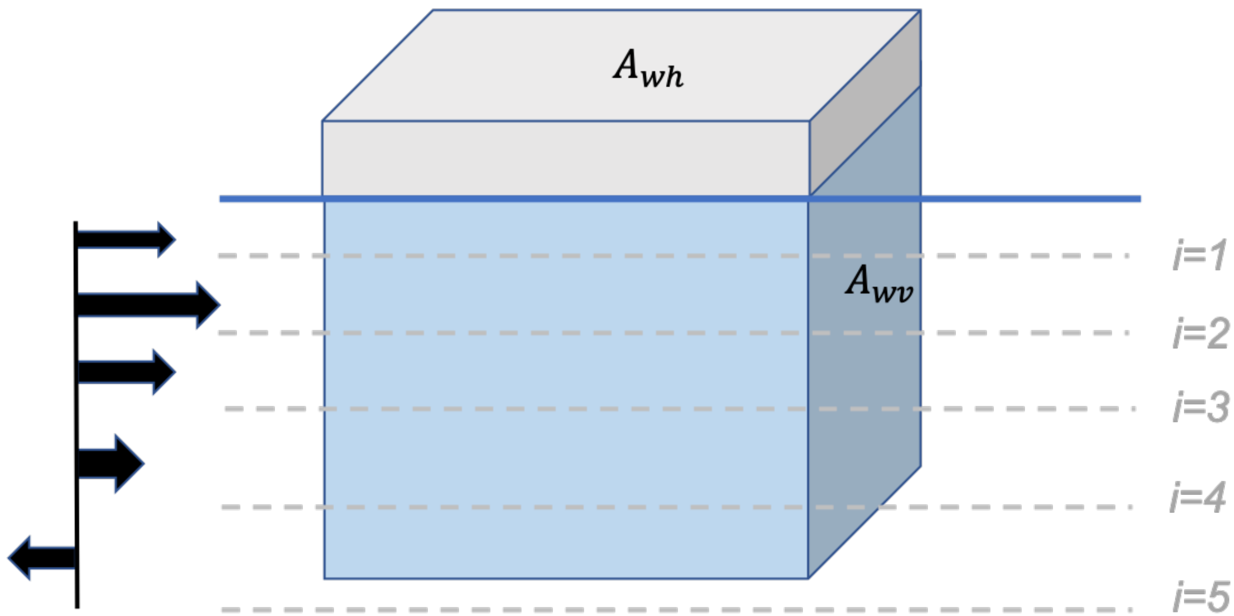


**Supplementary Figure 2:** The multi-level keel scheme used in the iceberg model to calculate ocean drag. In this example, the iceberg keel penetrates 5 vertical levels in the ocean model; flow in the top 4 levels is to the right of the page and to the left of the page in the bottom level. The net ocean drag exerted on the iceberg is the sum of all 5 levels.

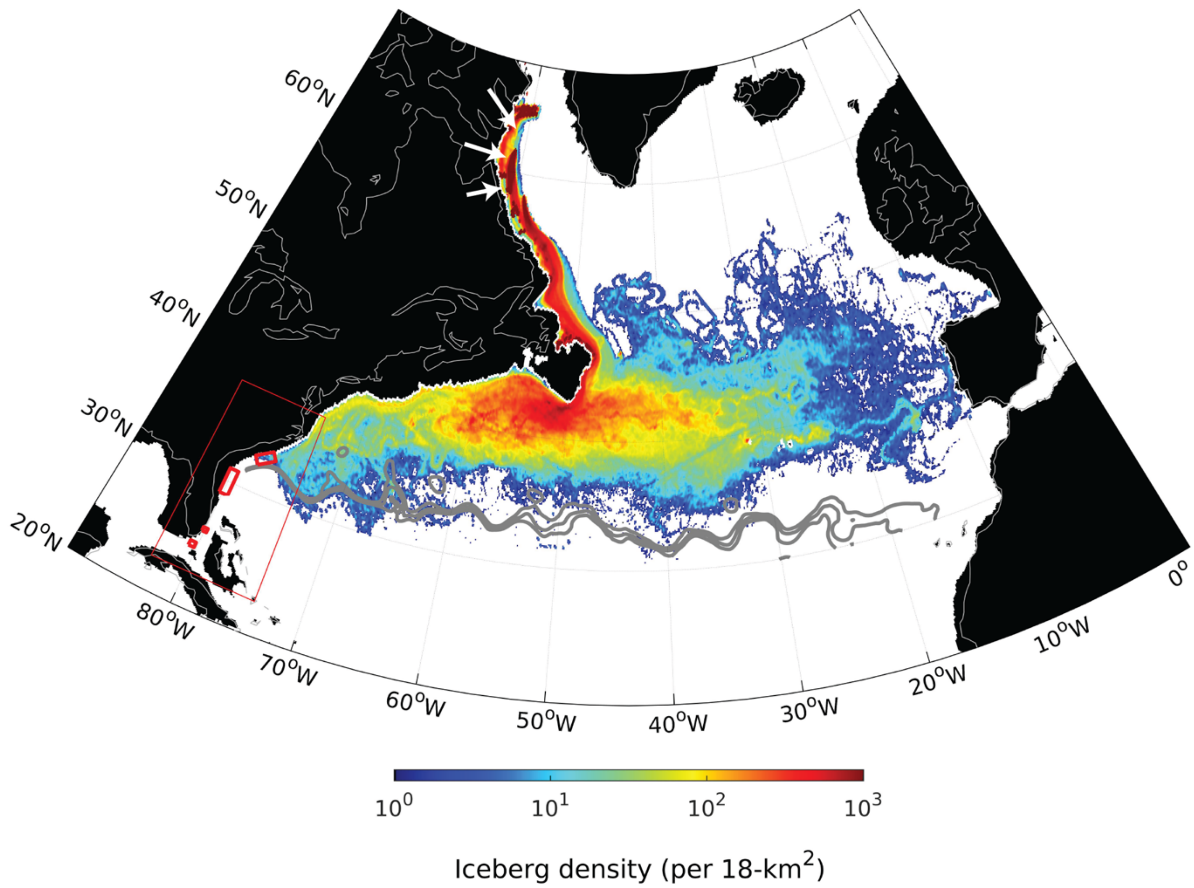


**Supplementary Figure 3:** The simulated distribution of icebergs in the glacial North Atlantic in response to a southward shift in the latitude of the Gulf Stream. Compared to the Control simulation (Fig. 5), a small number of icebergs drift to the most northern relic scour sites - located off the coast of South Carolina, USA - due to slope waters now flowing further south at Cape Hatteras. Icebergs were nevertheless still unable to reach the most southerly scour sites located off the coast of Florida that are directly beneath the northward flowing Gulf Stream. For reference, the Gulf Stream is marked by the 13-15°C isotherms at 200m water depth (grey contour lines). Iceberg calving margins near Hudson Bay are denoted by the white arrows, glacial landmasses are shown in black.

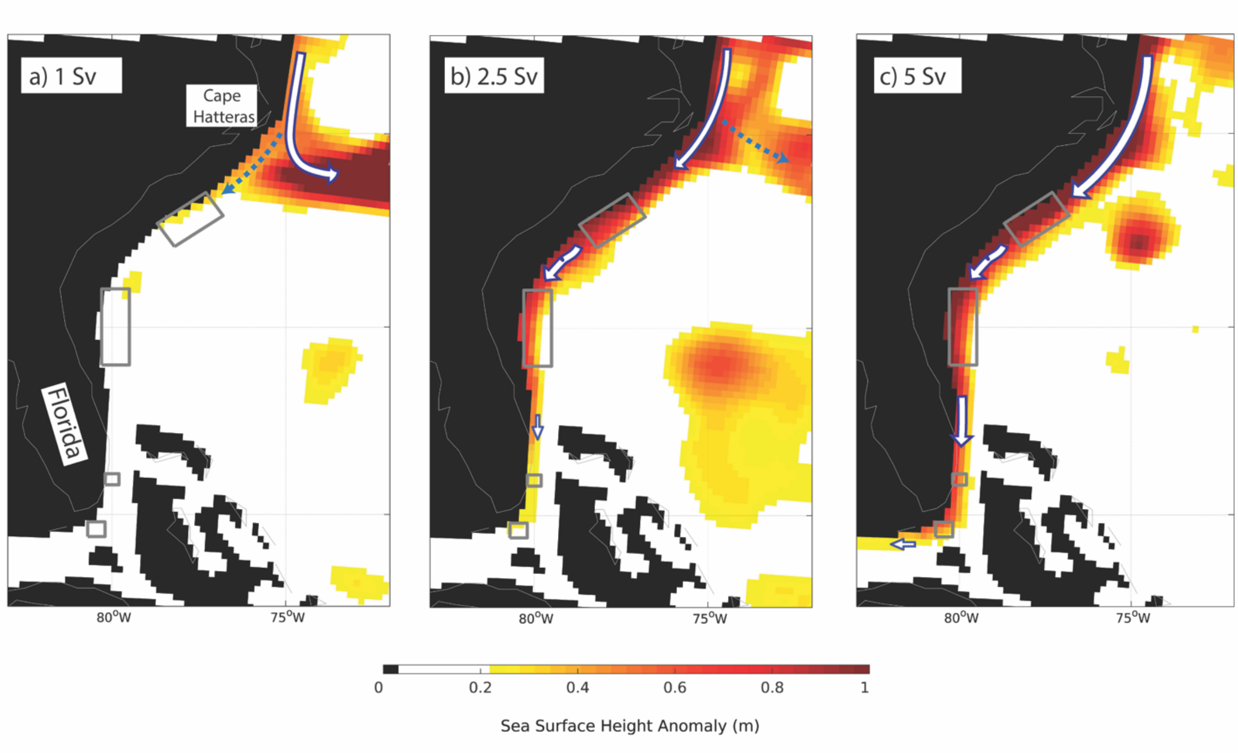


**Supplementary Figure 4:** Change in sea surface height in the subtropical western North Atlantic in response to elevated meltwater forcing from Hudson Bay, Canada. The panels (a-c) show the change in sea surface height (Perturbation minus Control) resulting from a 1 Sv, 2.5 Sv, and 5 Sv meltwater flood. The ability of the meltwater to flow south at Cape Hatteras, i.e. to 'overshoot', is dependant on whether the height of the meltwater exceeds the ambient sea surface height. This is the case for both the 2.5Sv and 5Sv meltwater floods, but not the 1Sv flood.

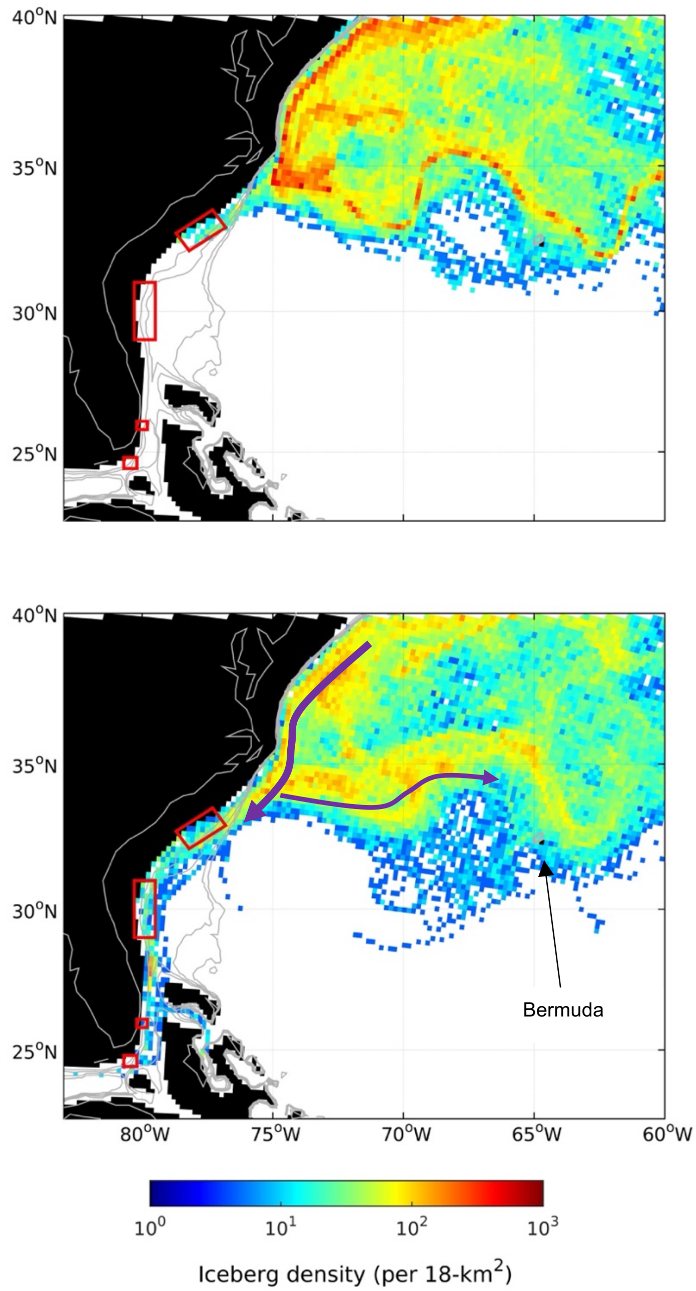


**Supplementary Figure 5:** Simulated iceberg drift patterns in the western subtropical North Atlantic. The maps show the mean density of icebergs for the first year of meltwater simulations with fluxes of 2.5 Sv (top) and 5 Sv (bottom). In the 2.5 Sv experiment, icebergs only reach the most northern relic subtropical scour sites off the coast of South Carolina; a flux of 5 Sv is required for icebergs to drift to the most southerly scours. The purple arrows (bottom panel) show the general drift directions of the icebergs: Initially, icebergs drift south along the eastern coast of the United States in the narrow coastal meltwater current; at Cape Hatteras a fraction of icebergs are retroflected eastward into the interior of the subtropical Atlantic gyre, with a significant number reaching Bermuda. In the 5 Sv experiment, icebergs continue drifting along the east coast of the USA, as far south as Florida Keys.

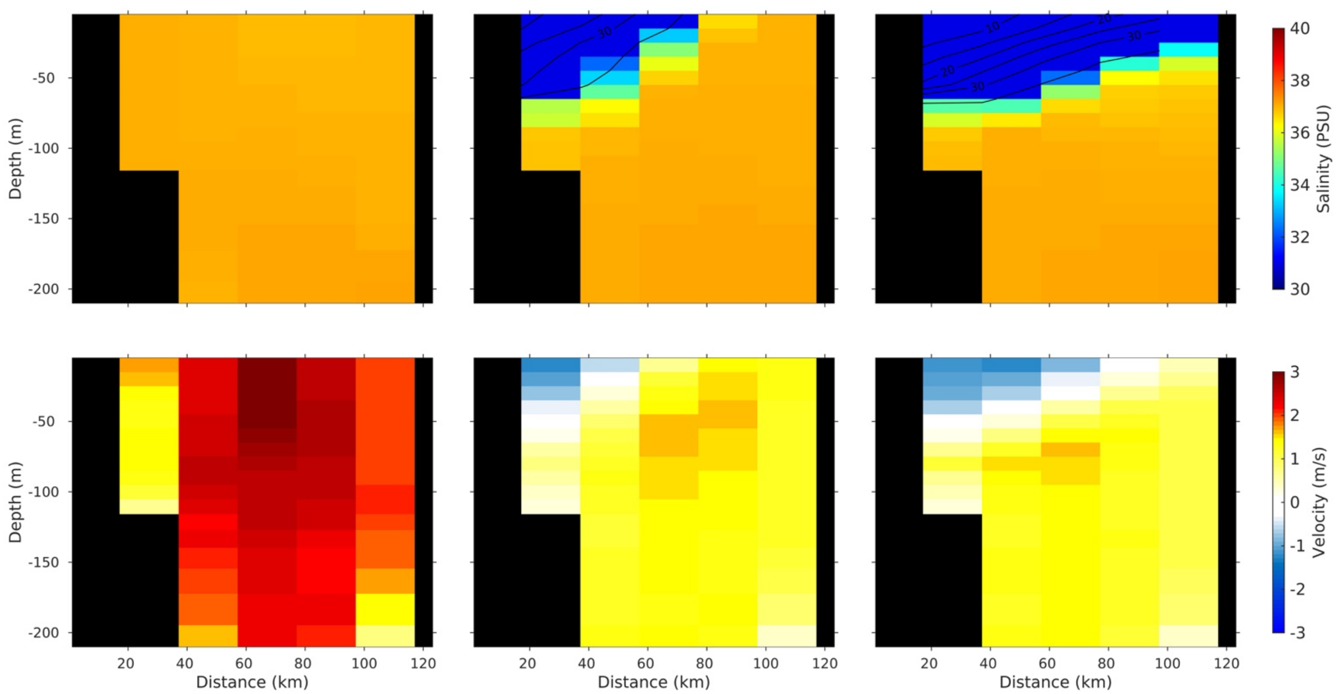


**Supplementary Figure 6:** Cross sections of salinity (top panels) and meridional (north-south) velocity (bottom panels) at Florida Strait (~26.5°N, 80°-78.5°W). The cross section is drawn as if the reader is looking north through the strait, such that the coast of Florida is on the left and Grand Bahama Island is to the right. The far-left panels show the salinity and flow in the Control, prior to the meltwater flood when flow is northwards at all depths. The two middle and two right panels show the ocean circulation in this region 90 and 300 days, respectively, after 5 Sv of meltwater was released from Hudson Bay.

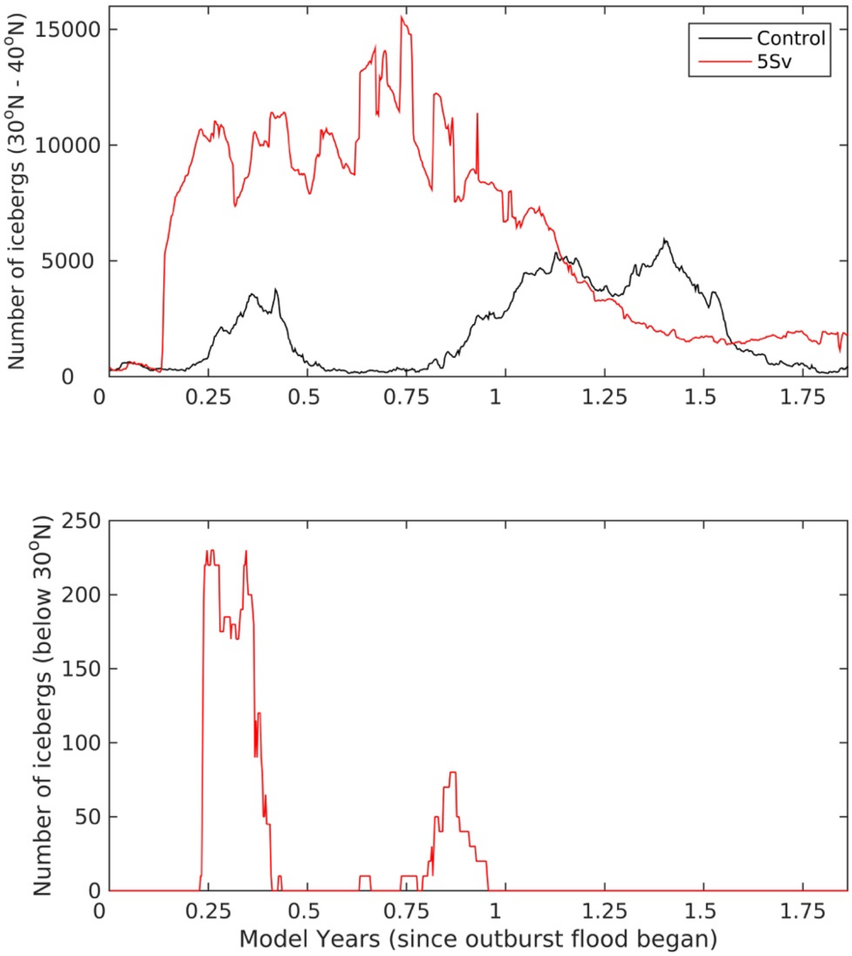


**Supplementary Figure 7**: Timeseries of the number of simulated icebergs in the North Atlantic between latitude bands 30° - 40°N (top) and below 30°N (bottom) in the Control and 5 Sv meltwater perturbation.

**Supplementary Table 1:** Radiocarbon ages for all samples used in this study.

| Core | Sample Depth (cm) | Sample Type | $^{14}C$ Age Yrs BP | Calendar Age Yrs BP | Heinrich Event* |
|---|---|---|---|---|---|
| 24GC | 68 | lithology changes | 11,830 ± 40 | 13,302 | **YD** |
| 24GC | 116 | | 15,300 ± 70 | 18,108 | |
| 24GC | 125 | | 27,150 ± 130 | 30,920 | H3 ~31,000 |
| 24GC | 129 | | 26,800 ± 280 | 30,646 | |
| 24GC | 150 | | 17,920 ± 50 | 20,180 | |
| 24GC | 152 | | 17,130 ± 50 | 21,154 | |
| 20GC | 106 | above scour | 24350 ± 90 | 27,990 | |
| 04GC | 116 | lithology change | 22,100 ± 140 | 25,949 | |
| 04GC | 120 | | 22,800 ± 120 | 26,697 | |
| 04GC | 124 | | 24,500 ± 140 | 28131 | |
| 04GC | 140 | above scour | 25,700 ± 250 | 29369 | H3 ~31,000 |
| 04GC | 142 | below scour | 28,500 ± 350 | 32014 | |
| 04GC | 144 | | 28,400 ± 350 | 31902 | |
| 02GC | 115 | lithology change | 24,600 ± 150 | 28231 | |
| 02GC | 116 | | 25,900 ± 170 | 29612 | |
| 02GC | 133 | lithology change | 24,000 ± 140 | 27717 | |
| 02GC | 135 | | 25,100 ± 160 | 28734 | |
| 02GC | 142 | above scour | 26,500 ± 280 | 30393 | H3 ~31,000 |
| 02GC | 145 | below scour | 29,000 ± 250 | 32624 | |
| 02GC | 160 | above scour | 28,500 ± 130 | 31846 | H4 38,000 |
| 02GC | 162 | below scour | 33,400 ± 230 | 37100 | |
| 02GC | 165 | | 42,300 ± 2800 | 45896 | |
| 27GC | 130 | above scour | 28,200 ± 570 | 31863 | H3 ~31,000 |
| 27GC | 133 | below scour | 29,600 ± 680 | 33249 | |
| 27GC | 208 | lithology change | > 45000 | | |
| 27GC | 210 | | > 49400 | | |
| 27GC | 218 | lithology change | > 45700 | | |
| 27GC | 220 | | > 45800 | | |
| 27GC | 225 | lithology change | 45,900 ± 2000 | | |
| 27GC | 226 | | 51,500 ± 3900 | | |
| 27GC | 235 | above scour | 47,400 ± 1200 | | H4 38,000 |
| 27GC | 236 | below scour | 35,000 ± 310 | 39118 | |
| 27GC | 240 | | 44,100 ± 830 | | |
| 03GC | 140 | lithology change | > 52,000 | | |
| 03GC | 142 | | > 52,000 | | |
| 03GC | 166 | above scour | 51,200 ± 5900 | | H5 45,000 |
| 03GC | 170 | below scour | 46,400 ± 3300 | | |
| 03GC | 174 | | 47,400 ± 3700 | | |

**nearest event in time - calendar ages from Hemming (2004)*

**Supplementary Table 2:** A list of the main coefficients used to derive iceberg motion.

| Coefficient | Description | Units | Value |
|---|---|---|---|
| $\rho_i$ | density of iceberg | kg/m$^3$ | 917 |
| $\rho_w$ | density of water | kg/m$^3$ | 1025 |
| $\rho_a$ | density of air | kg/m$^3$ | 1.2 |
| $\rho_s$ | density of sea ice | kg/m$^3$ | 910 |
| $C_{wv}$ | vertical drag coefficient for water | dimensionless | 1 |
| $C_{av}$ | vertical drag coefficient for air | dimensionless | 0.8 |
| $C_{sv}$ | vertical drag coefficient for sea ice | dimensionless | 1 |
| $C_{wh}$ | horizontal drag coefficient for water | dimensionless | 0.0012 |
| $C_{ah}$ | horizontal drag coefficient for air | dimensionless | 0.0055 |
| $g$ | Gravity | m/s$^2$ | 9.8 |

**Supplementary Table 3:** A list of the main iceberg thermodynamics coefficients and constants.

| Coefficient | Description | Units | Value |
|---|---|---|---|
| $\Gamma_i$ | latent heat of fusion of ice | J/kg | 3.33x10$^5$ |
| $T_i$ | Iceberg temperature | °C | -4 |
| $\alpha$ | Iceberg albedo | dimensionless | 0.7 |
| $k_a$ | Thermal conductivity of air (at 10°C) | J/s/m/K | 0.0249 |
| $k_w$ | Thermal conductivity of water (at 0°C) | J/s/m/K | 0.563 |
| $\upsilon_a$ | kinematic viscosity of air (at 10°C) | m$^2$/s | 1.46x10$^{-5}$ |
| $\upsilon_w$ | kinematic viscosity of water (at 0°) | m$^2$/s | 1.83x10$^{-6}$ |
| $D_a$ | thermal diffusivity air (at 0°C) | m$^2$/s | 2.16x10$^{-5}$ |
| $D_w$ | thermal diffusivity water (at 0°C) | m$^2$/s | 1.37x10$^{-7}$ |
| $R$ | Roughness height of the iceberg | m | 0.01 |
| $W_p$ | Wave period | s | 6.2 |

**Supplementary Table 4:** Iceberg size distribution used in the model simulations.

| Size Class | Fraction (%) | Width (m) | Thickness (m) |
|---|---|---|---|
| 1 | 15 | 67 | 80 |
| 2 | 15 | 133 | 160 |
| 3 | 20 | 200 | 240 |
| 4 | 15 | 267 | 320 |
| 5 | 8 | 333 | 360 |
| 6 | 7 | 400 | 360 |
| 7 | 5 | 500 | 360 |
| 8 | 5 | 600 | 360 |
| 9 | 5 | 800 | 360 |
| 10 | 5 | 1000 | 360 |